



SOUR GAS PIPELINE FAILURE DUE TO THE INTERACTION OF METHANOL WITH PRODUCED WATER

Russell Watts, P. Eng., Dr. Alex Tatarov, P. Eng. and Frank Gareau, P. Eng.
Skystone Engineering

Richard Leon, P. Eng.
Nexen Inc.

Copyright 2010 NACE International

Requests for permission to publish this manuscript in any form, in part or in whole must be in writing to NACE International, Publications Division, 1440 South Creek Drive, Houston, Texas 77084-4906.

The material presented and the views expressed in this paper are solely those of the author(s) and not necessarily endorsed by the Association. Printed in Canada

SOUR GAS PIPELINE FAILURE DUE TO THE INTERACTION OF METHANOL WITH PRODUCED WATER

Russell Watts, P. Eng., Dr. Alex Tatarov, P. Eng. and Frank Gareau, P. Eng.
Skystone Engineering
330, 4311 – 12th Street NE
Calgary, Alberta T2E 4P9
Canada

Richard Leon, P. Eng.
Nexen Inc.
2900, 801 – 7th Avenue SW
Calgary, Alberta T2P 3P7
Canada

ABSTRACT

A sour gas pipeline failed as a result of pitting corrosion initiated from the internal surface. The pipeline was pigged and treated with a batch corrosion inhibitor on a monthly basis. A continuous corrosion inhibitor program was also in place. The internal surface of the three kilometer long pipeline was in relatively good condition except for three significant single pits. Each pit penetrated 90% or more of the wall thickness. The magnetic flux leakage (MFL) inspection performed 17 months prior to the failure did not find pits deeper than 25% of the wall thickness.

Numerous corrosion mechanisms were considered, including CO₂ corrosion, H₂S corrosion, corrosion due to elemental sulfur, aqueous corrosion enhanced by NaCl, stray current (AC or DC) corrosion, galvanic corrosion, microbiologically influenced corrosion (MIC), and corrosion due to organic acids.

The interaction between produced water and methanol contributed to the failure. The results of this investigation and corrosion mitigation enhancements are reviewed.

Keywords: sour gas, produced water, methanol, sodium chloride, internal pitting corrosion, inhibition, in-line inspection, MFL tethered tool

INTRODUCTION

A 114.3 mm nominal, 4.0 mm thick carbon steel pipeline failed in November 2007. The pipeline transported sour gas, hydrocarbon condensate and produced water from an upstream wellhead to a main pipeline gathering system three kilometers away.

The pipeline was installed in 2002 and constructed of CSA Z245.1 Grade 359 Category 1 material. It had a maximum operating pressure (MOP) of 5520 kPa. The pipeline right-of-way (ROW) was parallel to a group of overhead transmission power lines.

The well produced 22.0 E³m³/d of gas and 0.6 m³/d of hydrocarbon condensate. The composition of the produced fluids showed concentrations of 9.38% H₂S and 9.40% CO₂ gases plus 617 ppm of chloride ions (Cl⁻) in the produced water. Additional elemental analysis found polysulfides in low concentrations less than 100 ppm.

From its commissioning, the pipeline was pigged and batch inhibited with a corrosion inhibitor on a monthly basis. A methanol slug (minimum of 100 L) would be pushed through the pipeline by a cup and multi-disk cleaning pig. The pig was followed by the batch of corrosion inhibitor. Well production pushed the entire batching train. Methanol was used to control hydrates that would form in the pipeline during pigging that would have prevented the movement of the batching train. A continuous corrosion inhibitor program was also in place to supplement the batch corrosion inhibitor program.

The line pipe was externally coated with mill-applied black polyethylene tape wrap beneath a layer of insulation (25.4 mm thick) and covered with black extruded high-density polyethylene (HDPE). Cathodic protection was provided by an impressed current system. Monthly rectifier readings showed that the current output from the rectifiers met or exceeded the minimum target for the pipeline to be protected. Annual pipe-to-soil potential readings also indicated adequate cathodic protection.

Three in-line inspections of the pipeline using magnetic flux leakage (MFL) tethered tools were completed in 2004, 2006 and 2007. The in-line inspection results from 2004 noted one anomaly at 26% wall loss near the wellhead. The second in-line inspection did not identify any indications greater than 25% wall loss, which was the minimum reporting standard. The final in-line inspection of the pipeline was completed immediately after the leak was discovered in 2007 to determine the failure location. The MFL tethered tool revealed 27 anomalies greater than 25% wall loss. Three of the anomalies were reported on the in-line inspection log to be greater than 90% wall loss. Two of these anomalies were excavated near the wellhead. The other was one kilometer further downstream in the pipeline.

INVESTIGATION PROCEDURE

The MFL tethered tool detected two pits near the upstream wellhead following the pipeline leak: Pit 1 at 55.28 m (98% wall loss) and Pit 2 at 46.60 m (89% wall loss). Three line pipe cut-out samples corresponding to the in-line inspection segment from 43.50 m to 59.28 m downstream of the wellhead were provided for analysis. The cut-outs were examined visually and chemical spot tests were performed. Corrosion deposits were collected and examined by X-ray diffraction (XRD). Cleaned samples were examined using optical microscopy and scanning electron microscopy (SEM) techniques. Elemental compositions at different locations were determined by an energy-dispersive X-ray spectroscopy (EDS) technique.

A separate field investigation was initiated. The investigation included a review of the in-line inspection history for the pipeline an evaluation of the pipeline corrosion mitigation and monitoring programs plus an examination of the well production history. Soil analyses found significant concentrations of NaCl near the leak site.

The laboratory analysis and field investigation results were then correlated to determine the factors that contributed to the damage mechanism.

RESULTS

Visual Examination

Visual Examination of Cut-out Containing Through-Wall Pit 1 at 55.28 m.

A pinhole opening initiating from the internal pipe surface was discovered at the 5 o'clock position at 55.28 m, where a 98% deep pit was observed by in-line inspection. Pit 1 was circular in shape and 12 mm in diameter. The pit was not filled with corrosion deposit; and just a thin layer of a black corrosion deposit was still adherent to the pit walls. The edges of the pit were smooth and rounded. Figure 1 shows the external and internal surfaces of through-wall Pit 1.

The external polyethylene coating was not compromised and found to be in good condition. The external surface of the pipe was in good condition and not affected by corrosion. The foam insulation was cracked and soaked with hydrocarbon fluid indicating the leak location. The external surface around the pit opening was also in good condition and minimally affected by corrosion.

Visual Examination of Cut-out Containing Pit 2 at 46.60 m.

The straight line pipe cut-out section from 43.50 m to 49.60 m contained an in-line inspection indication corresponding to an 89% wall loss pit located at the 46.60 m mark, at the 6 o'clock position. The internal surface of the pipe was covered with a shiny oily layer and contained a pit close to the 46.60 m mark, at the 5 o'clock position (see Figure 2). The internal surface of the pipe between the 7 and the 8 o'clock positions was affected by general corrosion (see Figure 3).

The external polyethylene coating was not compromised and in good condition. The foam insulation under the polyethylene coating was dry, with no hydrocarbon stain, in close to brand-new condition. The external surface of the pipe was in good condition and contained no pit opening.

The internal surface of the pipe was covered with a non-uniform black layer. At numerous locations, both at the top and at the bottom, the layer was compromised, and corrosion initiated.

The main pit was located close to the 46.60 m mark. It was round, 12 mm in diameter and located at the 5 o'clock position. The pit was 3.8 mm deep, which corresponded to 95% of the wall thickness. This pit was similar in geometry to the pit at 55.28 m, which suggests similar pitting/corrosion mechanism.

The pit contained a small amount of deposit on its walls. The upper layer of the deposit was yellowish, and the bottom layer was blackish. The difference in color may indicate a difference in the chemical composition. The deposit from the pit shown in Figure 2 was collected for X-ray diffraction examination.

Figure 3 shows the area between the 7 and the 8 o'clock positions which was affected by general corrosion, observed as shallow elongated interconnected corroded areas. The biggest observed area was 460 mm long and 20 mm at the widest part.

Chemical Spot Tests

Test results on the internal surface were positive for sulfides (which is consistent with the presence of H₂S) and negative for carbonates. Test results for chlorides were positive for the unwashed line pipe as well as inside the pits, and negative for the line pipes after they were solvent cleaned.

A copper sulfate test performed away from the pits and the groove was negative indicating the presence of a protective layer on the internal pipe surface.

X-ray Diffraction (XRD)

Prior to cleaning the line pipe cut-out samples, deposits from Pit 2 at 46.60 m and from the area of general corrosion were removed and analyzed by XRD.

Figure 4 shows the XRD results, and Figure 5 shows an elemental analysis of the deposit within the Pit 2 at 46.60 m. The material generated a moderate quality diffractogram indicating the sample is composed of both crystalline and non-crystalline compounds. X-ray diffraction analysis shows the crystalline components of the sample are composed of 58% formation fines, 18% iron sulfide scale or corrosion products, 15% salt, 6% calcium carbonate scale, 3% barium sulfate and 1% iron oxide corrosion products. Elemental analysis suggests the presence of non-crystalline iron and chlorine bearing compounds.

Figure 6 shows the XRD results, and Figure 7 shows an elemental analysis of the deposit from the area affected by general corrosion. The material generated a good quality diffractogram indicating the sample is mainly composed of crystalline compounds. XRD analysis shows the crystalline components of the sample are mainly composed of iron sulfide scale or corrosion products (about 80%). Elemental iron, formation fines and iron oxide corrosion products occur at minor to moderate volumes.

Scanning Electron Microscopy / Energy Dispersive Spectroscopy Examination

Two cross-sections were prepared from two pits:

- A circumferential cross-section through Pit 1 at 55.28 m.
- A longitudinal cross-section through the secondary Pit 2 at 46.60 m.

Examination of the SEM/EDS results revealed the following:

- Elemental composition of the base metal corresponded to a carbon steel with approximately 1% Mn and 0.3% Si. Such a composition is expected for CSA Z245.1 Grade 359 material.
- The internal surface of the line pipe in good condition was covered with a layer of iron oxide, which is potentially a mill scale.
- Corrosion pits developed in the areas where the iron oxide layer was compromised.
- Small pits were completely filled with corrosion deposit.
- Large pits contained deposit only close to their walls. This may indicate aggressive pitting.
- Corrosion deposit mostly consisted of iron sulfides.
- Some pits also contained a notable amount of iron oxides and/or iron hydroxides (SEM/EDS examination could not distinguish between iron oxides or iron hydroxides).
- No indications of elemental sulfur inside the pits were observed.

Figures 8 through 11 are SEM images. They show different stages in pit development.

- Stage 1: Uncorroded pipe.
- Stage 2: The internal surface was covered with an oxide layer (mill scale). The oxide layer developed breaks. Chloride ions are known as a potential scale penetration.
- Stage 3: Corrosion pits began to form under the breaks. Small pits were filled with corrosion deposit.
- Stage 4: The oxide layer was not present after the pits grew. Corrosion deposit was near and parallel to the pit surface.

- Stage 5: Large pits contained small amounts of corrosion deposit close to their walls.

Metallographic Examination

Metallographic examination revealed that:

- The line pipe exhibited ferrite microstructure with traces of pearlite, which is typical for CSA Z245.1 Grade 359 low-carbon steel.
- The microstructure was similar close to and far away from the pits.
- There were no metallurgical defects which could result in accelerated pitting.

DISCUSSION

Based on the historical and current results of water and gas analyses, and discussion with field operations personnel, the following corrosion processes could potentially take place in the pipeline

- CO₂ corrosion
- H₂S corrosion
- Corrosion due to elemental sulfur
- Aqueous corrosion enhanced by NaCl
- Stray current (AC or DC) corrosion
- Galvanic corrosion
- Microbiologically influenced corrosion (MIC)
- Corrosion due to organic acids

CO₂ Corrosion

Neither spot test nor XRD examination revealed the presence of iron carbonates. The shape of the pits was not typical for CO₂ corrosion attack. Thus, CO₂ corrosion was discarded as a major corrosion mechanism. Nevertheless, it may play a minor role as a contributing factor to corrosion failure.

H₂S Corrosion

XRD found that iron sulfides constitute the major part of the corrosion deposit. Spot testing, SEM/EDS analysis and elemental mapping all confirmed the presence of iron sulfides. Iron sulfides were found at the bottom of all corrosion pits, and the shape of the corrosion pits did correspond to H₂S corrosion attack. Thus, H₂S corrosion was considered to be the major corrosion mechanism.

Corrosion due to Elemental Sulfur

XRD analysis of corrosion deposits did not find elemental sulfur. An extensive examination of content of major and minor pits on the metallographic cross-section did not find elemental sulfur. A well-site water analysis performed in March 2005 showed less than 100 ppm polysulfides. Corrosion by elemental sulfur was excluded as a reason for the failure.

Aqueous Corrosion Enhanced by NaCl

XRD analysis found 14.8% NaCl in the deposit inside Pit 1, which is a significant quantity. The presence of NaCl was confirmed by the EDS analysis. NaCl was likely chemically deposited in the pit. NaCl promotes pitting corrosion and could result in an auto-catalytic corrosion process within a confined pit environment. Elemental mapping found iron oxides/iron hydroxides in early stages of pit formation. NaCl promotes the formation of iron hydroxides.

Stray Current (AC or DC) Corrosion

There was no external corrosion observed on the analyzed sections of the pipeline. The external polyethylene coating contained no visible holidays. The corrosion damage on the internal surface was located far away from flanges so there was no driving force for the current leaving the metal and going into the electrolyte. Thus, stray current corrosion was discarded as a corrosion mechanism.

Galvanic Corrosion

Galvanic corrosion occurs due to difference in chemical composition of the electrically connected electrodes immersed in electrolyte. The examination showed that there could be two galvanic couples which could result in pitting corrosion:

- Fe (bare metal inside the pit) – anode, iron sulfide scale – cathode.
- Fe (bare metal inside the pit) – anode, iron oxide scale – cathode.

Both galvanic couples will result in an accelerated pitting corrosion, and the pit should be clean, which is typical for galvanic corrosion. Two major corrosion pits were almost empty; they contained a small amount of iron sulfide corrosion products adjacent to walls. In order for galvanic corrosion to start, a protective layer should be broken, exposing the bare metal, after which the galvanic corrosion becomes self-supporting. Figures 8 through 11 shows different stages in pit growth, including breaking of the protective layer of iron oxide. Galvanic corrosion was considered to be a significant contributing factor in corrosion failure.

Microbiologically Influenced Corrosion (MIC)

Corrosion pits due to MIC corrosion usually have specific morphology, such as pit-in-pit formation and/or terracing. Often secondary pits are developed in close proximity downstream from main pits due to bacteria transported by flow. The morphology of the observed corrosion damage did not correspond to a bacterial attack. A biological activity reaction test (BART) for bacteria was run in triplicate on a wellhead fluid sample. The test did not indicate the presence of the bacteria. Thus MIC corrosion was discarded as a corrosion mechanism.

Corrosion due to Organic Acids

Organic acids, such as acetic or formic acid, are often used in oil and gas well-stimulation treatments. Inhibited organic acids are much less reactive with metals than are hydrochloric acid or mixtures of hydrochloric acid and hydrofluoric acid. If organic acids came inside the pipeline, they could potentially result in the breaking of the protective layer and subsequent pitting corrosion.

Root Cause Analysis

The internal pipe surface had a protective layer that consisted of three distinct layers:

- Iron oxide (mill) scale closest to the surface (see Figure 8).
- Iron sulfide layer revealed by spot testing. The layer was not observed either by SEM or under a metallographic microscope, which indicates that the layer was thin.
- Inhibitor film.

The iron oxide mill scale is hard, but also brittle. It will crack with time when stressed or from mechanical impact, thus exposing the base metal. Chloride ions can also cause scale breakdown.

The iron sulfide layer was likely thin and it could become less protective in the presence of either NaCl or CO₂.

Thus, the inhibitor film is deposited on top of the iron oxide and iron sulfide layers. The inhibitor film is absorbed on the iron oxide or iron sulfide layer with a low bond strength and can be removed by flow, and therefore it requires replenishing.

Corrosion damage could not take place without breaking the inhibitor film. As was discussed earlier, corrosion damage near the 46.60 m location demonstrated two different modes; pitting corrosion and general corrosion. The protective iron oxide/iron sulfide scale contained indications of multiple breaks. This is consistent with breaking of the inhibitor film:

- Corrosion pits initiated where the break in the inhibitor is localized. The pit was 12 mm in diameter and 3.8 mm deep, which corresponded to 95% of the wall thickness.
- General corrosion develops where the break takes place over a significant distance. A 0.5 m long and 20 mm wide corrosion groove was observed between the 7 and the 8 o'clock positions.

Several factors could result in the breaking of the inhibitor film:

- Flow regimes such as slug flow that produce high shear stresses near the pipe wall.
- Insufficient thickness of the film due to lack of inhibitor added.
- Removal of the inhibitor film by chemical means such as methanol washing.

Reportedly, both analyzed pits were located on an uphill slope, which promotes a slug flow regime. Slug flow results in high levels of shear and turbulence at the bottom of the pipe, which strips away the protective films formed on pipe walls resulting in high corrosion rates.

A conservative corrosion control program was in place for the 114.3 mm pipeline and was consistently followed. Monitoring results showed the inhibitor was added to the pipeline in sufficient quantity, as recommended by the chemical vendor.

A large slug of methanol was pushed through a sour gas pipeline with the intent of controlling the formation of dangerous hydrates during routine cleaning pig operations. Methanol could act as a solvent to the inhibitor film, reducing its thickness or removing it entirely from the pipe wall.

Methanol is also highly miscible in water and if injected in large volumes it can lower the solubility of ionic salts, such as sodium chloride (NaCl), causing them to precipitate out of solution. A high concentration (14.8%) of NaCl was in the pit deposit and in the soil near the leak. Water analysis showed 617 mg/L of NaCl, and the amount of water in the condensate was small. The large volume of methanol added to the pipeline during pigging operations precipitated salt that was present out of solution. The NaCl then reacted with the iron sulfide layer that had been left unprotected by the removal of the inhibitor film. The presence of ionic salts promoted pitting corrosion within carbon steel pipelines and resulted in an autocatalytic galvanic corrosion process within the confined pit environment.

CONCLUSIONS

The pipeline failed as a result of pitting corrosion initiated from the internal surface. The pit at the 55.28 m location penetrated the entire wall thickness, and the pit at 46.60 m location penetrated 95% of the wall thickness. In-line inspection identified the depth and locations of the major pits with good accuracy.

Pitting corrosion was a result of a combined action of H₂S, NaCl and galvanic corrosion. CO₂ corrosion, stray current corrosion, corrosion due to elemental sulfur, and microbiologically influenced corrosion did not contribute significantly to the failure.

The slug of methanol in front of routine pigging was a contributing factor in the corrosion mechanism. The large volume of methanol acted as a solvent and removed the protective inhibitor film from the pipe wall. Methanol, being highly miscible in water, lowered the solubility of NaCl in solution and caused it to precipitate. The NaCl then reacted with the iron sulfide layer initiating the development of the pit. An autocatalytic galvanic corrosion reaction then continued eventually causing the through-wall pit.

Field methanol practices should be incorporated into the development of corrosion mitigation practices including laboratory tests to select the corrosion inhibitor.

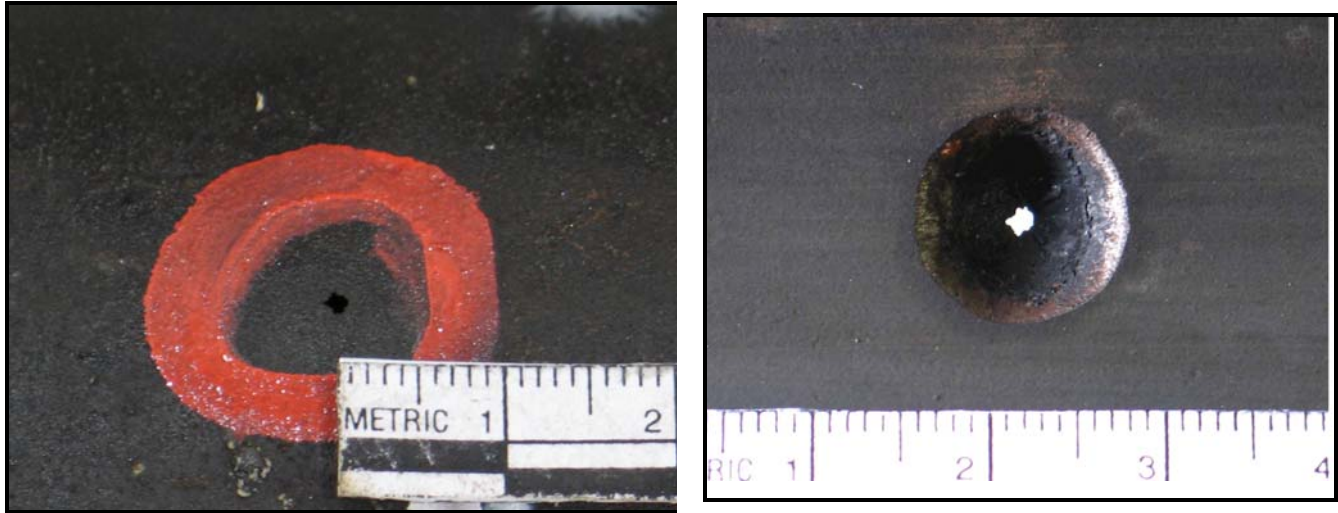


FIGURE 1 – External and Internal Surfaces of Through-wall Pit 1 at 55.28 m

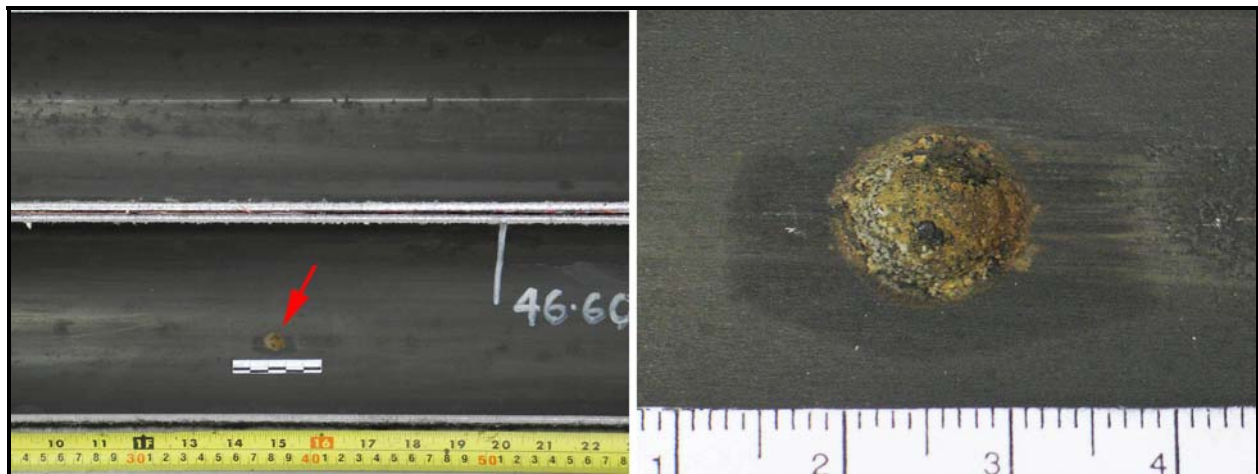


FIGURE 2 – Pit 2 at 46.60 m Under Different Magnifications

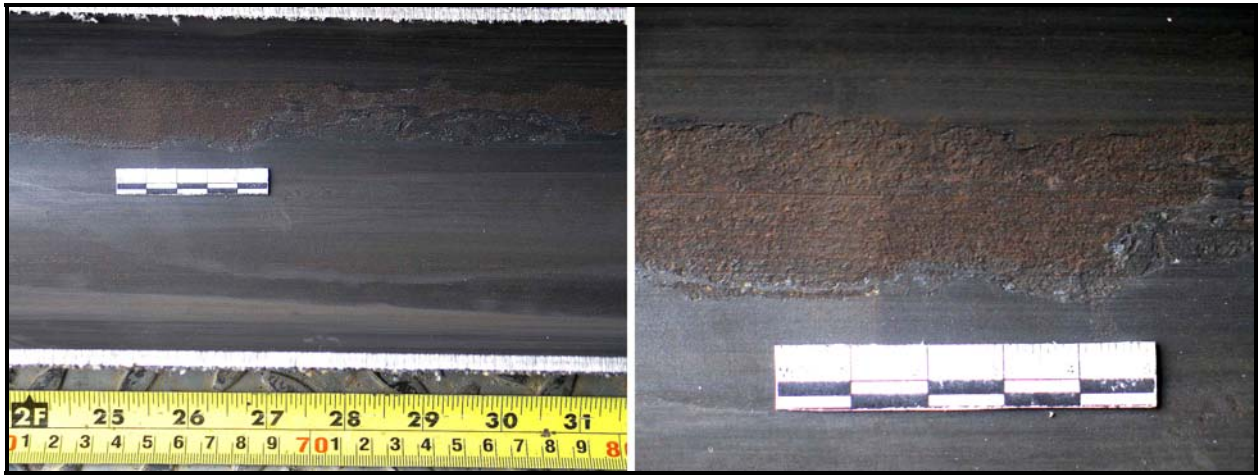


FIGURE 3 – General Corrosion On Internal Surface Between 7 and 8 O'clock Positions

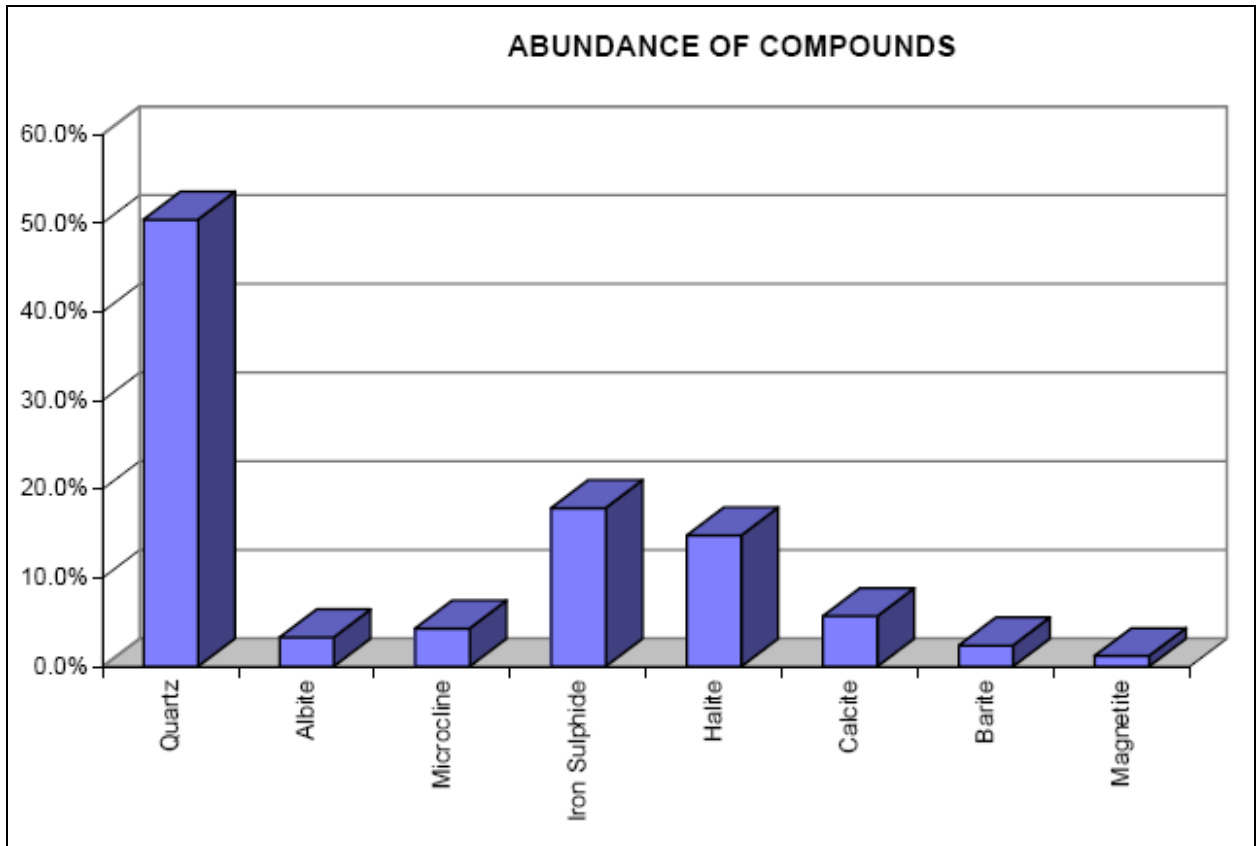


FIGURE 4 – XRD Results from Pit 2 at 46.60 m

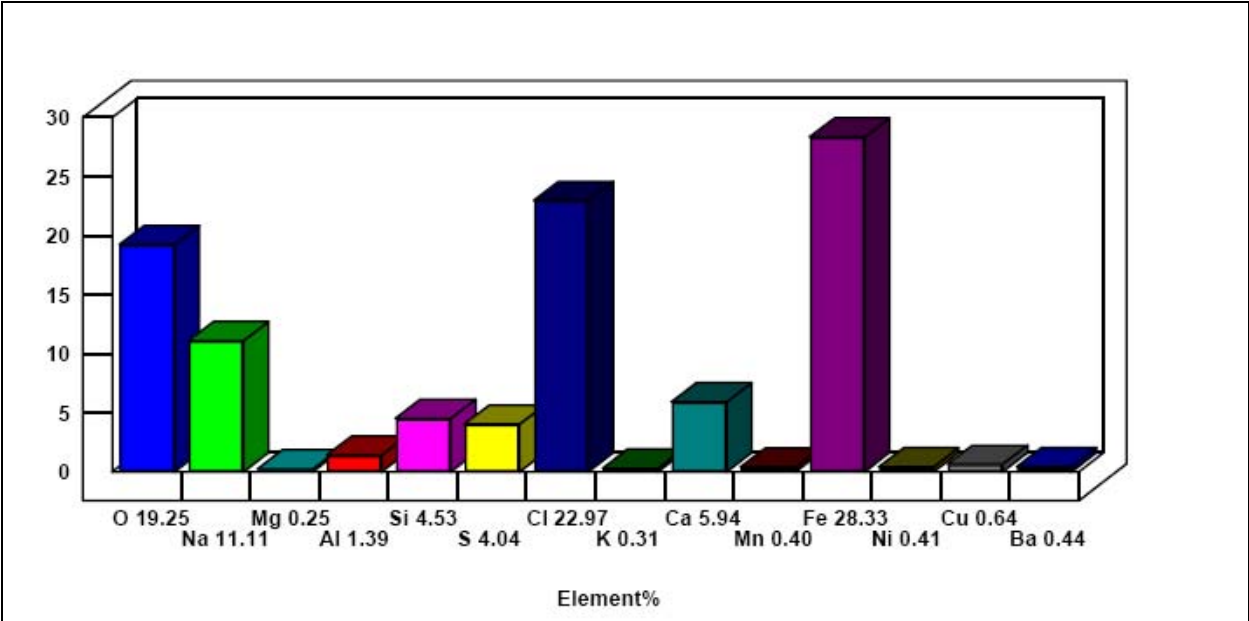


FIGURE 5 – Elemental Analysis of Deposit in Pit 2 at 46.60 m

ABUNDANCE OF COMPOUNDS

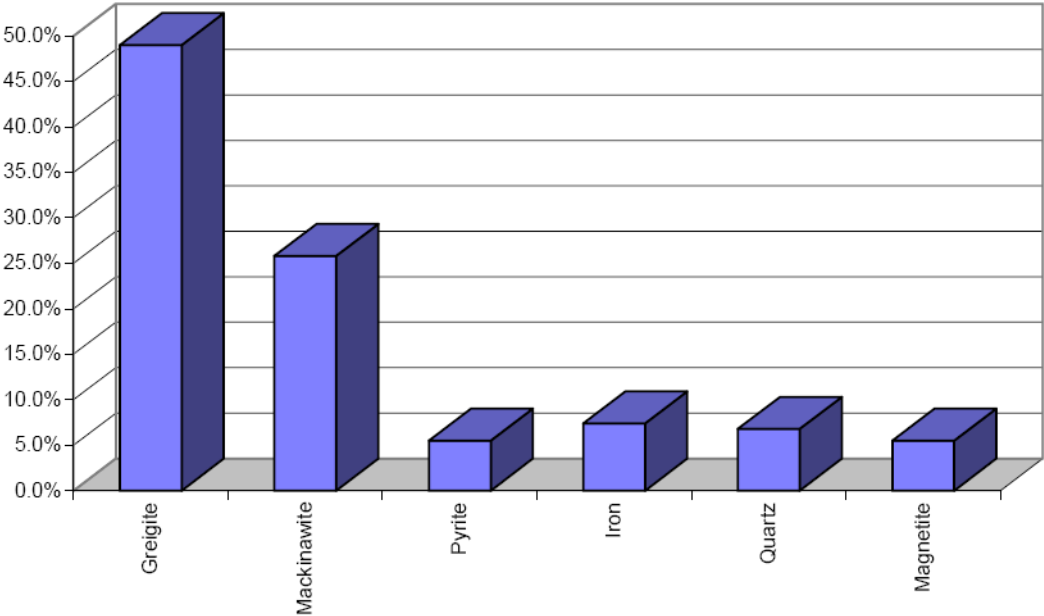


FIGURE 6 – XRD Results from the Area of General Corrosion

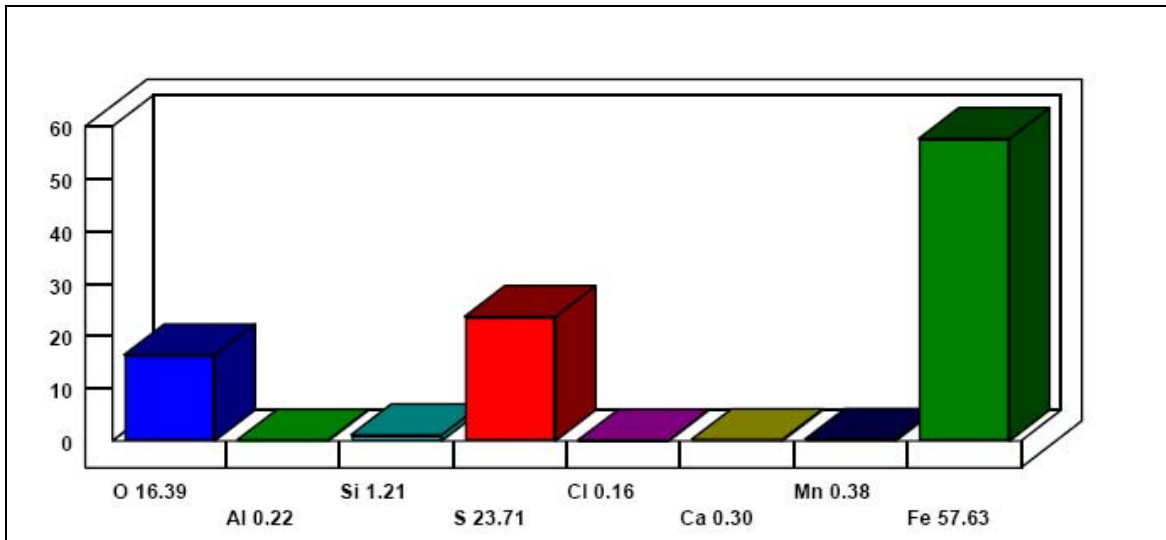


FIGURE 7 – Area of General Corrosion Elemental Analysis

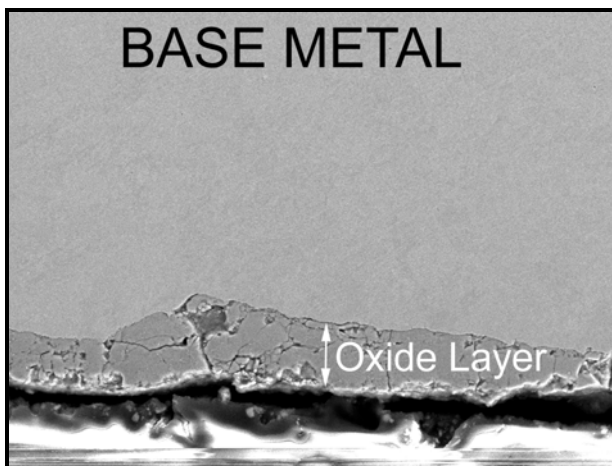


FIGURE 8 – Stage 2: Breaks In Oxide Layer.
Mag. 1000X

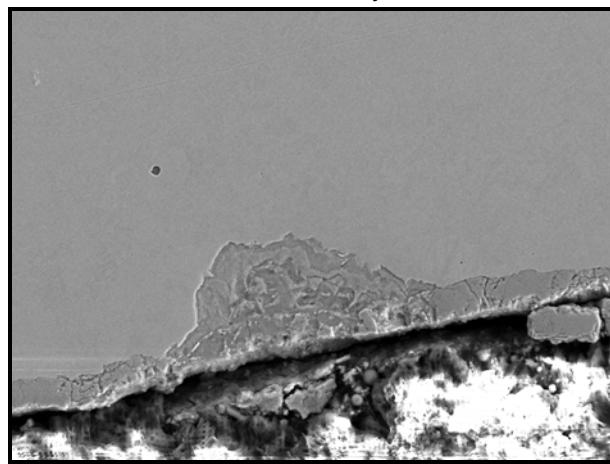


FIGURE 9 – Stage 3: Formation Of Small Pit
below The Breaks in The Oxide Layer.
Mag. 750X

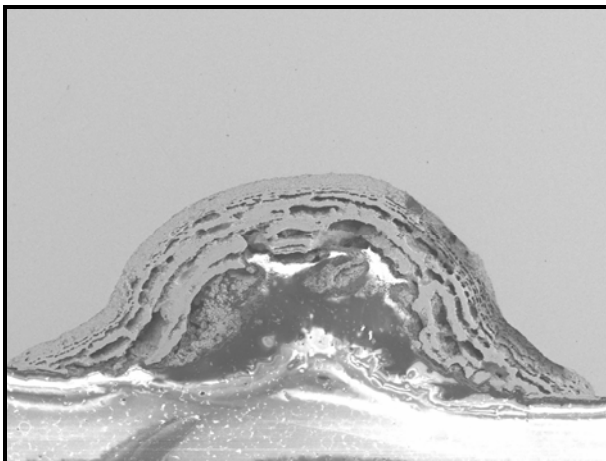


FIGURE 10 – Stage 4: Bigger Pits Are Partially
Filled With Deposit. Mill Scale Not Present.
Mag. 40X

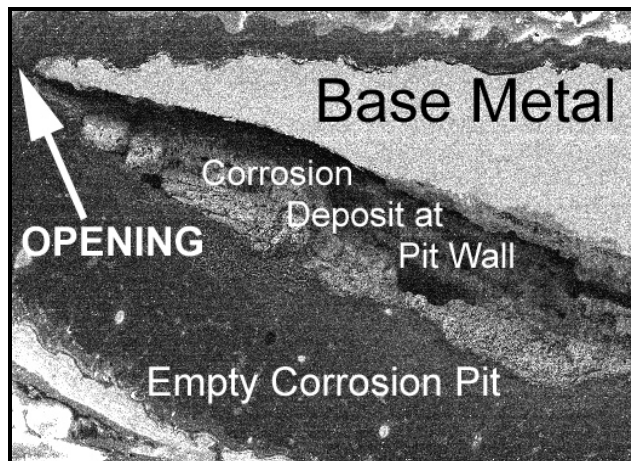


FIGURE 11 – Stage 5: Large Pits Are Almost
Empty. Mag. 70X